

## Study of Synthetic Clay Minerals. III.<sup>1)</sup> Synthesis and Characterization of Two Dimensional Talc

Noriyuki TAKAHASHI,\* Masanori TANAKA, Teiji SATOH, and Tadashi ENDO†

Mizusawa Industrial Chemicals, Ltd., Nakajo-machi, Niigata 959-26

† Department of Molecular Chemistry and Engineering, Faculty of Engineering, Tohoku University, Aramaki, Aoba, Sendai 980

(Received May 20, 1994)

“Two dimensional” talc was prepared by the hydrothermal reaction of various silicas with magnesium hydroxide. The precipitated and activated silicas were especially available as starting materials. The powder X-ray diffraction data indicated that the resulting talc consisted of no-stratified and random layered structure. According to the IR spectrum, no solid acidity, i.e. Brønsted and Lewis acid sites were found. The specific surface area was over  $500 \text{ m}^2 \text{ g}^{-1}$ . A large amount of water was adsorbed and partially combined with the surface of lamellar talc. As a result, the artificial talc would receive applications such as emulsifying agents to the mixture of liquid paraffin and water.

Many investigations have been done on the synthesis of talc in the system  $\text{MgO-SiO}_2\text{-H}_2\text{O}$ . Mitsuda and Taguchi<sup>2)</sup> reported that the magnesium silicate hydrate were synthesized at  $180^\circ\text{C}$  for 8 weeks or at  $400^\circ\text{C}$  for 4 h. Muraishi<sup>3)</sup> showed that the talc was formed from magnesium hydroxide and silica via serpentine by the hydrothermal reaction in which crystalline silica was put on the bottom and magnesium hydroxide crystals were hung from the top of reaction container filled with water. The main purpose of these reports would be done to obtain the well crystallized talc under the conditions of high temperature and long reaction duration, and to understand the mineralogical crystallization mechanism.

There are major industrial uses for talc, for instance, the natural crystallized talc is used as a filler for paper in large quantities. The filler called by “weathered talc”, which has good hydrophilicity, is much useful as a pitch control agent in paper making process. In the food industry, new talcs are recently expected as adsorbents, bearing mild surface activity for purifying raw materials of foods with favorable flavor and taste.

In this paper, the synthesis of non-stratified and micro-crystalline talc and its chemical adsorption characteristics were systematically examined.

### Experimental

**Materials.** The precipitated silica ( $\text{SiO}_2 \cdot n\text{H}_2\text{O}$ ) and the Japanese acid clay were of Mizusawa Industrial Chemicals, Ltd., Japan, the pyrogenic silica (AEROSIL 200), the colloidal silica (Snowtex 30), and magnesium hydroxide were purchased from Nippon Aerosil Co., Ltd., Nissan Chemical Industries, Ltd., Wako Pure Chemical Industries, Ltd., (Japan), respectively. The activated silica was prepared by leaching the Japanese acid clay with sulfuric acid solution.<sup>4)</sup>

**Synthesis of the Two Dimensional Talc.** A portion of 200 g precipitated silica in suspension (corresponding to 0.5 mol of  $\text{SiO}_2$ ) and 22 g of magnesium hydroxide (corresponding to 0.38 mol of  $\text{MgO}$ ) were intimately mixed in  $370 \text{ cm}^3$  of distilled water. The slurry was charged into a TEM-V 1000 type-autoclave with the capacity of  $1 \text{ dm}^3$

(supplied by the Taiatsu Co.) kept at  $160^\circ\text{C}$  for 5 h under stirring at 500 rpm. The vapor pressure was equilibrated at about 0.6 MPa under conditions described above. After cooling, the slurry was filtered and then dried at  $130^\circ\text{C}$ . The total amount of resulting sample (referred to compound 1) was 51.1 g. The other samples (referred to compounds 2, 3, and 4) were synthesized by using activated, colloidal and pyrogenic silicas as starting materials, respectively.

**Analysis.** IR spectra of synthesized talcs were measured by a Nihon-Bunko A-302 Spectrometer using KBr method. X-Ray powder diffraction (XRD) patterns were measured by a Rigaku Denki Geiger Flex using Ni-filtered  $\text{Cu K}\alpha$  radiation at the scanning rate of  $2\theta/2^\circ \text{ min}^{-1}$ . Differential thermal analysis (DTA) and thermogravimetry (TG) were measured by a Rigaku Denki TG-DTA/S apparatus. All the analyses were carried out under conditions of a heating rate of  $10^\circ\text{C min}^{-1}$  and an air flow rate of  $50 \text{ cm}^3 \text{ min}^{-1}$ . The specific surface area ( $S$ ) and the pore volume ( $V$ ) were determined by a nitrogen adsorption method using a Carlo Erba Soaptomatic Series 1800. The surface areas were calculated by the BET equation. Densities ( $\rho$ ) were determined by a Helium Pycnometer 1302-02 of Micromeritics Instr. Co. The acidic properties were evaluated from IR spectroscopy of the sample chemisorbed pyridine.<sup>5)</sup>

**Observation of Emulsification.** A portion of 20 g water and 20 g liquid paraffin were poured into a  $50 \text{ cm}^3$  glass bottle, and then the 0.4 g of sample was added thereto. The capped glass bottle was shaken for 15 min. using a ‘paint shaker’ supplied by Red Devil Inc. After standing for 24 h in an ambient atmosphere, the uniformity of resulting liquid was observed.

### Results and Discussion

**XRD.** Figure 1 shows the typical powder X-ray diffraction pattern of compound 1. The profile quite resembles to that of natural talc<sup>6)</sup> with some characteristics given as below. The number of peaks is so smaller than that of natural talc and those intensity are weak. Accordingly, it was clear that the crystallinity of the recovered talc was low. Four peaks were substantially assigned as  $(020, 11\bar{1})$ ,  $(13\bar{2})$ ,  $(24\bar{4}, 138)$ , and  $(060, 33\bar{2})$  planes. The half width of each diffraction

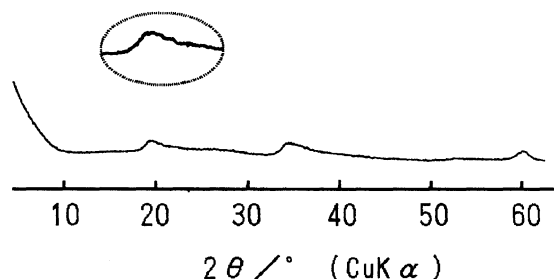


Fig. 1. XRD powder pattern of the compound **1**. One of the asymmetric peaks was magnified in the ellipse.

peak is so wide that the particles are small in size and strained. The small-angle X-ray scattering is observed on the side of low angle so that the compound **1** is possibly agglomerates consisting of many crystallites. No diffraction peak of (002) plane is observed. This indicates that little or no stacking of talc unit layer occurs. Since all peaks show asymmetric profile tailing towards higher angles, it was considered that the compound **1** is substantially composed of random layer structure.<sup>7)</sup> In addition, a halo figure is observed in the range  $2\theta=22^\circ$  to  $32^\circ$ , indicating the presence of amorphous silica.

Figure 2 shows the lower angle XRD patterns of the compounds **1** and **3**, both of which were obtained from different silica sources. The basal reflection of compound **1** is completely diminished. On the other hand, very weak peak is observed in compound **3**, corresponding to the basal spacing of ca. 1.1 nm. Also, the inten-

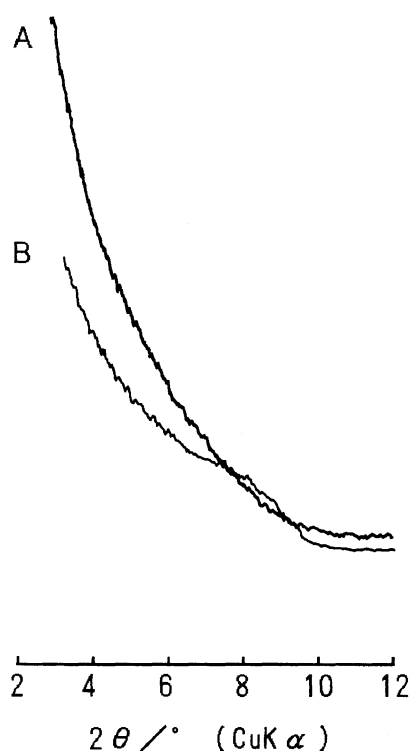
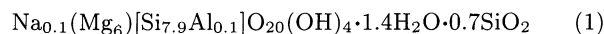


Fig. 2. XRD powder patterns of basal reflection: A is precipitated silica (the compound **1**) and B is colloidal silica (the compound **3**) as a silica sources.

sity of compound **3** is weaker than that of compound **1** in a small-angle X-ray scattering. Such observation suggests that the crystallinity of compound **3** is higher than that of compound **1**.

**Chemical Analysis.** Table 1 shows the results of the chemical analysis of compound **1**. Each ingredient was indicative of the following chemical composition; corresponding to the talc with  $\text{O}_{20}(\text{OH})_4$  unit.



Excess amount of silica, which did not contribute to form talc structure, was expressed in this formula. Small amounts of Al and Na components were also analyzed. Such elements were involved as impurities in the precipitated silica as starting material. In addition,  $\text{Si}^{4+}$  seemed to be partially replaced by  $\text{Al}^{3+}$  in the silicate layers of the talc structure.<sup>8)</sup>  $\text{Na}^+$  ion was positioned into the gallery between silicates for keeping the electroneutrality. However, it was ambiguous whether or not the formulated water belonged to the composition of talc and amorphous silica.

**IR.** The IR spectrum of compound **1** is shown in Fig. 3. The IR spectrum reveals that the compound **1** is identified as natural talc<sup>9)</sup> classified into 2:1 type clay minerals rather than natural antigorite<sup>10)</sup> classified into 1:1 type clay minerals. The peak at  $3680\text{ cm}^{-1}$ , corresponding to the  $\nu$  mode of isolated OH group in octahedral layer of natural talc, is not found but an intense and broad peak at  $3410\text{ cm}^{-1}$ , corresponding to

Table 1. Chemical Analysis of the Compound **1**

Component	wt%	Element	Atomic ratio <sup>a)</sup>
$\text{SiO}_2$	62.10	Si	8.6
$\text{Al}_2\text{O}_3$	0.39	Al	0.1
$\text{Fe}_2\text{O}_3$	0.02	Fe	0.0
MgO	29.08	Mg	6.0
CaO	0.27	Ca	0.0
$\text{Na}_2\text{O}$	0.41	Na	0.1
Ignition loss	7.23	H	6.8
Total	99.50		

a) Based on  $\text{O}_{20}(\text{OH})_4$ .

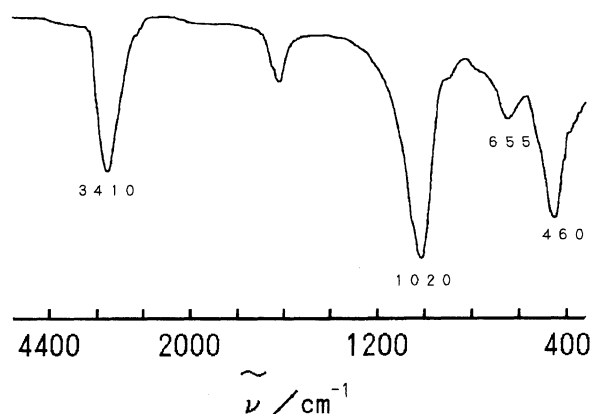


Fig. 3. IR spectrum of the compound **1**.

the  $\nu$  mode of polymeric OH group, is observed in the IR spectrum of the compound **1**. This result suggests that the OH group in the octahedral layer is not isolated, but linked by a hydrogen bond to the adjacent adsorbed water in the talc structure. Consequently, the compound **1** seems to be tiny crystallites with few layer stacking.

**Thermal Analysis.** In the DTA curve shown in Fig. 4, an exothermic peak starting at 830 °C is observed. This peak is participated in the transformation of talc to enstatite. An endothermic peak with the weight loss of 11% is observed upto 150 °C. This peak seems to arise from the release of water adsorbed physically on the lamellar surface of talc. In addition, the mild endothermic peak in the temperature range 400 to 700 °C is attributed to the elimination of the constituent water. On heating at 700 °C, the weights of compounds **1** and **3** are decreased upto 93 and 95% against the initial ones obtained at 150 °C, respectively.

**Products Dependence on the Mole Ratio of Mg/Si.** Figure 5 shows the IR spectra of the products obtained by using "activated silica", and with the various mole ratio of Mg/Si ( $K$ ) in the range of 1.6/8 to 12/8.

Between 1.6/8 and 6/8 of the  $K$ ; as the quantity of silica lowered, the absorption peaks are decreased at 1100 and 795  $\text{cm}^{-1}$  and increased at 1000, 910, and 650  $\text{cm}^{-1}$ , indicating the formation of talc. The proportion of the conversion to talc is probably governed by the quantity of MgO in reactants. The compound **2** (at 6/8 of  $K$ ) shows almost the same spectra as the compound **1** with the shoulder around 780  $\text{cm}^{-1}$ , indicative of the presence of quartz. The quartz impurities, which is involved in starting material, might have lower reactivity with magnesium hydroxide than the activated silica.

Between 6/8 and 12/8 of the  $K$ , the absorption peak at 3600  $\text{cm}^{-1}$ , characteristic of the  $\nu$  mode of OH in magnesium hydroxide, disappeared even at higher  $K$

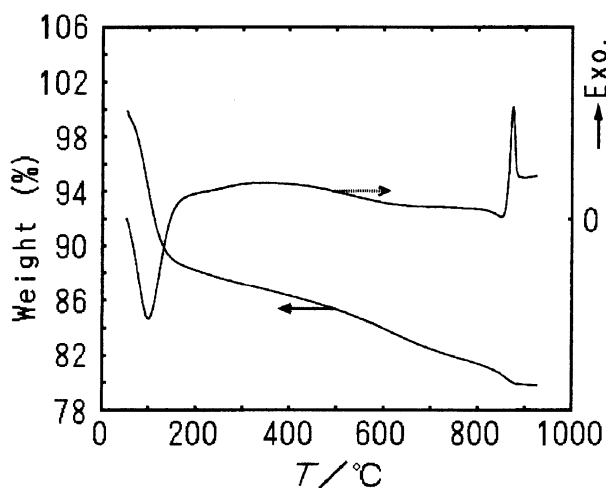


Fig. 4. TG-DTA curves of the compound **1**.

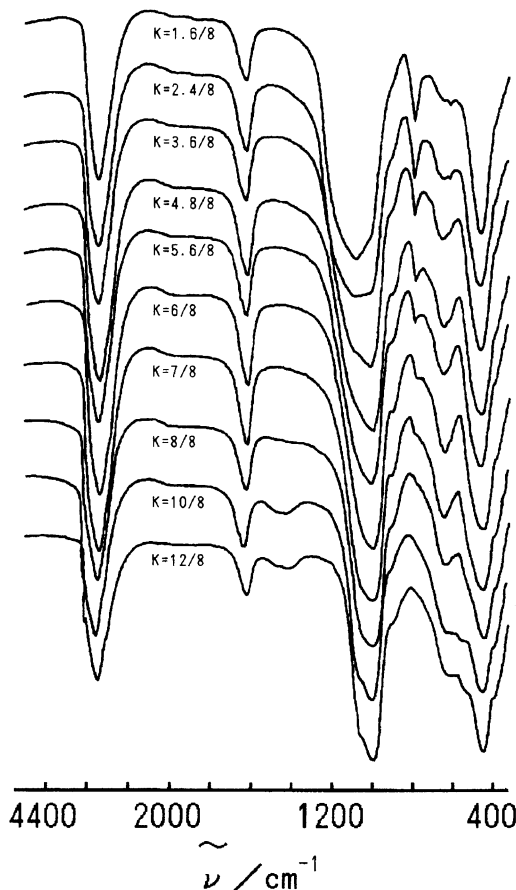


Fig. 5. IR spectra of products prepared by various Mg:Si mol ratio ( $K$ ), where silica is an activated one.

than 6/8 of  $K$  in talc. The absorption peaks of the products were decreased at 650  $\text{cm}^{-1}$  and increased at 1075, 615, and 560  $\text{cm}^{-1}$  in intensities, indicative of the formation of 1:1 type serpentine mineral. All the results suggested that the  $K$  of reactants was significant to determine either type of clay minerals, 2:1 or 1:1.

**Nitrogen Adsorption.** The compound **1** has 642  $\text{m}^2 \text{g}^{-1}$  of  $S$  and 2.6  $\text{g m}^{-3}$  of  $\rho$ . Assuming that the shape of crystallite is rectangular of which the lateral faces are minimized, the thickness of crystallite ( $D_s$ ) is simply estimated by the Eq. 2. The values of  $D_s$  for compounds **1** and **4** are calculated to be 1.2 and 2.7 nm, respectively. The small figures are compatible with the observation of small-angle X-ray scattering.

$$D_s = \frac{2}{\rho \times S}. \quad (2)$$

**Heat-Resisting Property.** Figure 6 shows the specific surface area ( $S$ ) and the pore volume ( $V$ ) of the compound **1** calcined at each temperature. It is obvious that the bound water is successively lost in the temperature region shown in TG curve. The apparent changes of  $S$  and  $V$  are 17 and 6% in the range of 150 and 700 °C. If normalized by the quantity of the constituent water given at 150 °C, these values were equivalent to 23 and 12%, respectively.

Table 2. Infrared Wavenumber of Pyridine and Its Relatives

Sample	Wavenumber/cm <sup>-1</sup> <sup>b)</sup>					
Adsorbed on the compound <b>1</b>	1636w	1626w	1607s	1544w	1490s	1422s
Hydrogen-bonded <sup>a)</sup>		1614	<u>1593</u>		1490	1438
Pyridinium <sup>a)</sup>	<u>1638</u>	1620		<u>1545</u>	1490	
Co-ordinated <sup>a)</sup>		1620	1577		1490	<u>1450</u>

a) Ref. 10. b) Underlined wavenumbers indicate the key peak for identification. s: Strong. w: Weak.

Table 3. Characteristics of the Synthetic Talcs Obtained by Using Various Silicas

No.	Silica Source			Product		
	State of silica	Ig. loss wt%	<i>S</i> m <sup>2</sup> g <sup>-1</sup>	<i>S</i> m <sup>2</sup> g <sup>-1</sup>	<i>V</i> cm <sup>3</sup> g <sup>-1</sup>	Liquid Profile
1	Precipitated	2.94	177	642	0.92	Emulsified
2	Activated	3.94	303	575	0.45	Emulsified
3	Colloidal	2.46	176	281	0.34	Separated
4	Pyrogenic	1.74	201	286	0.41	Separated

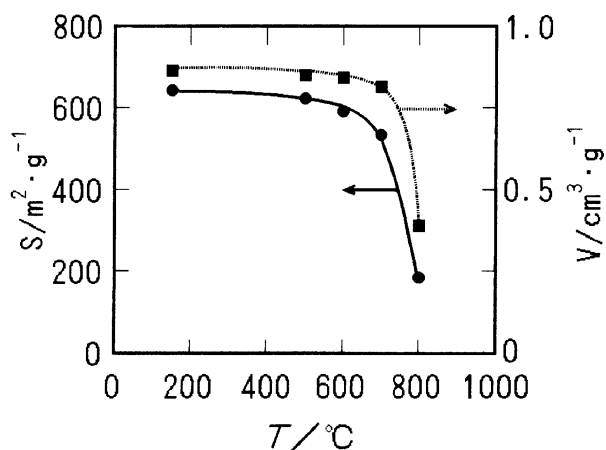


Fig. 6. Specific surface area (*S*) and pore volume (*V*) of the compound **1** obtained after calcination.

The nitrogen adsorption isotherm was of B.E.T type for the compound **1** calcined at every temperatures. This mean that the porous characteristic was conserved up to 700 °C. On the other hand, the large decreases of the *S* and the *V* took place between 700 and 800 °C. Noted that two-dimensional characteristics of compound **1** collapsed above 800 °C. The observation was due to the conversion from talc to enstatite.

**Pyridine Absorption.** The IR spectra of the pyridine adsorbed on the compound **1** are measured upon heating at various temperatures. Table 2 lists the IR peaks of the sample treated at 120 °C with that of pyridine in three different bonding states.<sup>11)</sup> The observed IR peaks are identified as the hydrogen bonded pyridine with a trace of pyridinium ion. The absorption intensities of the hydrogen bonded pyridine are decreased with

increasing the temperatures between 120 and 500 °C, and the weight of sample was decreased to about 13% after IR spectroscopic measurement. As described in the term of Thermal Analysis, the physically adsorbed water was fairly released upon 200 °C. In consequence, the absorbed pyridine was likely bonded by a hydrogen bonding to the adsorbed water. On the other hand, the intensity of pyridinium ion was scarcely decreased in the temperature range of TG-DTA analysis. Brønsted acid sites, bringing about pyridinium ion, may be produced by the combination of the constituent water and Lewis acid sites which was induced by substituting of Al<sup>3+</sup> for Si<sup>4+</sup> in the silicate layers of talc.

**Emulsification Phenomenon.** A natural talc is known to be lipophilic and hydrophobic. It was found that the compounds **1** and **2** were readily emulsified in a mixture of oil and water (see Table 3). The emulsification phenomena of the compound **1** was closely related to the bound water shown in the formula (1) and 11 wt% of adsorbed water resulting from porous characteristics as shown in Fig. 6.

**Reactivity of Silica.** The *S* and the emulsification ability of the compounds **1** to **4** were fairly dependent on the kind of silica source as starting material. Such dependences failed to be understood on the basis of the ignition loss and *S* of silica source (Table 3). Since amorphous silica reacts readily with magnesia in hot water to form Si–O–Mg bonding, the silica as starting materials of the compounds **1** and **2** is almost the same as “amorphous silica” in reactivity. It is, therefore, considered that the reaction progressed rapidly only to form the talc unit layer. No more significant change was recognized in the XRD pattern of the compound **1** during the further reaction of 20 h. Especially, the remains

of non-reacted silica were apparent. Muraishi<sup>3)</sup> demonstrated that silica reacted stepwise and gradually with magnesia to provide well-crystallized serpentine or talc. The compounds **3** and **4** exhibited higher crystallinity and lipophilicity than the compounds **1** and **2**. It is expected that the "colloidal" and "pyrogenic" silicas have lower reactivity than the "precipitated" and "activated" silicas. Under the present reaction conditions, the stratification of talc unit layers was completed by using "crystallized silica" as starting material.

**Structure Model.** The compound **1** is probably composed of 1 or 2 unit layers which are made of two silica tetrahedral sheets with a central magnesia octahedral sheet. This result was proven by the  $D_s$  value of 1.2 nm, while the thickness of talc layer is 0.9 nm.<sup>12)</sup> According to the observations of the asymmetric XRD peaks, the compound **1** also consists of the random layer structure with the different orientation in plane. Also, the micro-silicas with various particle sizes are probably contributed to forming the agglomerates at random.

On the other hand, the compound **3** showed the existence of basal spacings with weak intensity and a small-angle X-ray scattering. In consequence, the compound **3** seems to resemble not to two dimensional talc but kerolite,<sup>13)</sup> which shows occasionally both asymmetric reflection and basal reflection, indicating the stratification of 3 or 4 parallel-layers.

The authors thank Dr. Takeo Wada of Mizusawa

Industrial Chemicals Ltd. (Niigata) and Professor Masahiko Shimada and Dr. Fuxue Jin of Tohoku University (Sendai) for useful discussions.

## References

- 1) Part II; N. Takahashi, M. Tanaka, and T. Satoh, *Nippon Kagaku Kaishi*, **1991**, 692.
- 2) T. Mitsuda and H. Taguchi, *Cem. Concr. Res.*, **7**, 223 (1977).
- 3) H. Muraishi, *Bull. Chem. Soc. Jpn.*, **54**, 878 (1981).
- 4) Y. Sugawara, *Kogyo Kagaku Zasshi*, **69**, 209 (1966).
- 5) K. Mizuno, M. Ikeda, T. Imokawa, J. Take, and Y. Yoneda, *Bull. Chem. Soc. Jpn.*, **49**, 1788 (1976).
- 6) JCPDS file No. 13-558.
- 7) J. Kakinoki, K. Katada, and T. Hanawa, *Acta Crystallogr.*, **13**, 448 (1960).
- 8) A. Léonard, S. Suzuki, J. J. Fripiat, and D. De Kimpe, *J. Phys. Chem.*, **68**, 2608 (1964).
- 9) V. Stubican and R. Roy, *Am. Mineral.*, **46**, 32 (1961).
- 10) S. Simoda, "Nendo Kobutu Kenkyu Ho," Sozosya, Tokyo (1985), p. 152.
- 11) M. R. Basila, T. R. Kantner, and K. H. Rhee, *J. Phys. Chem.*, **68**, 3197 (1964).
- 12) H. P. Klug and L. E. Alexander, "X-Ray Diffraction Procedures," John Wiley and Sons, New York (1954), p. 517.
- 13) G. W. Brindley and G. Brown, "Crystal Structures of Clay Minerals and Their X-Ray Identification," Mineralogical Soc., London (1980), p. 167.